A Wide-band Millimeter Wave RWG to Air-Filled SIW Transition

Muhmmad Shah Alam[#], Khalid AlMuhanna[#], Asif Alam[$], Haoran Zhang[^], Atif Shamim[^]

[#]Imam Mohammad Ibn Saud Islamic University, Saudi Arabia

[$]Delta International School, Saudi Arabia

[^]King Abdullah University of Science and Technology, Saudi Arabia

{malam, kalmuhanna}@imamu.edu.sa, asifsaquib748@gmail.com,

{haoran.zhang, atif.shamim}@kaust.edu.sa

Abstract— **In this paper, a simple linearly tapered transition from a rectangular waveguide (RWG) to an air-filled SIW (AFSIW) is designed by analytically formulating its length, which optimizes the impedance matching and insertion loss over the wide millimeter wave frequency range. Several of these transitions are used to realize back-to-back and transmission systems supporting different waveguides. Their performances in terms of S_{11} and S_{21} are simulated and found to be <-10 dB and >-0.21 dB across the frequency bands of operation, respectively. The prototype of the transition in transmission system configuration supporting the WR-15 waveguide is developed, and its measured values from 50 to 75 GHz correlate very well with the simulated results. When the measured S_{21} and BW of the developed prototype are compared to similar works reported in the literature, the benefits of the proposed transition are confirmed for developing low-cost future generations of wireless technology systems.**

Keywords— **Wideband, Millimeter Wave, Rectangular Waveguide, Air-Filled Substrate Integrated Waveguide (AFSIW), Tapered Transition**

I. Introduction

Various millimeter Wave frequency bands [1]-[2] are projected to be used by high-speed wireless and RADAR systems. These high-performance systems typically employ rectangular waveguides (RWGs) [3], but doing so makes the system bulky and costly. Thus, to reduce the cost, the use of air-filled SIW (AFSIW) is of high interest [4]-[6] as it offers low cost, reduced insertion loss, and high-power handling capability [5]. However, in these system scenarios, the AFSIW often needs to be interfaced with an external system that relies on the RWG format; therefore, a wideband low-loss RWG to AFSIW transition is a critical requirement.

The literature has extensively covered designing transitions [7]-[9]. The two main categories are in-line and right-angle layouts [7]. Although the design is complex in the former case, the substrate-integrated waveguide and the RWG have the same orientation, supporting parallel integration with large operational bandwidths. Contrarily, in the latter case, where the two axes are perpendicular, they meet through one or two coupling slots cut in the broad wall of the substrate-integrated waveguide but suffer from limited bandwidth because of the resonant structure [8]-[9].

The transition from RWG to AFSIW operating in the 15–22 GHz band [3] is developed using an in-line extension technique described in [7]. Moreover, the literature survey confirms that such transitions in the millimeter wave bands are not reported.

Therefore, in this work, a simple in-line RWG to AFSIW transition is proposed, which operates over a wideband with minimal insertion loss. The transition design is systematically developed in this work by following the procedure elaborated in flow chart, and its length is analytically derived, which optimizes the impedance matching and insertion loss (See Section III).

The paper is organized as follows. The design of AFSIW is described in Section II. Section III discusses the concept involved in the proposed transition and how its length is optimally used to achieve excellent impedance match and reduced insertion loss, and their values in different operating bands are summarized in Section IV. Section V shows the image of the developed prototype compatible with WR-15 and the measurement setup used. Discussions and comparison of measured with simulated results and conclusions are covered in Sections VI and VII, respectively.

II. Air-Filled SIW (AFSIW) Structure

The AFSIW [5] utilizes a multilayer PCB process, as shown in Fig. 1. The substrates 1 and 3 realize the conducting top and bottom surfaces, while substrate 2 is sandwiched in the middle, which contains an air-filled region W separated by a gap of dielectric slab w_1 and arrays of metallic vias on both sides of the substrate of height h. The cutoff frequency f_c of the wave traveling in the AFSIW satisfies Eq. (1), and its width W is determined as [10]:

$$\frac{\tan\left(\frac{w_1 \times \pi f_c \times \sqrt{\epsilon_r}}{c}\right)}{\sqrt{\epsilon_r}} = \cot\left(\frac{W \times \pi f_c}{c}\right) \qquad (1)$$

Where,

w_1 = Dielectric slab (PCB edge tolerance)

c = Velocity of light; ε_r = Dielectric constant; $W_f = W + 2w_1$

The W is determined using (1). After that, the diameter and separation between the center-to-center of the vias are determined using the technique described in [11]. Substrates 1 and 3 can be utilized to realize baseband or digital circuits for a more cost-effective wireless system solution.

III. The Concept of Proposed Transition

The aperture size of RWG (a and b) and AFSIW (W_f and h) decides the nature of the transition, either taper out or taper in.
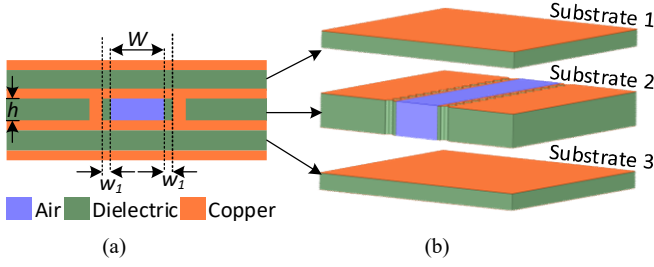
Fig. 1. AFSIW (a) Cross-sectional view (b) Different substrates

The equations of designing a taper in different configurations are expressed as:

$$y_{OUT} = a + (W_f - a)\left[1 - \left(1 - \frac{x}{L_1}\right)\right] \qquad (2)$$

$$h_{IN} = b + (h_t - b)\left[1 - \left(1 - \frac{x}{L_1}\right)\right] \qquad (3)$$

$$h_{OUT} = b + (h_t - b)\left[1 - \left(1 - \frac{x}{L_1}\right)\right] \qquad (4)$$

The plot for these equations is shown in Fig. 2(a)-(c). The different tapered design options are described in the design flow chart given in Fig. 3.
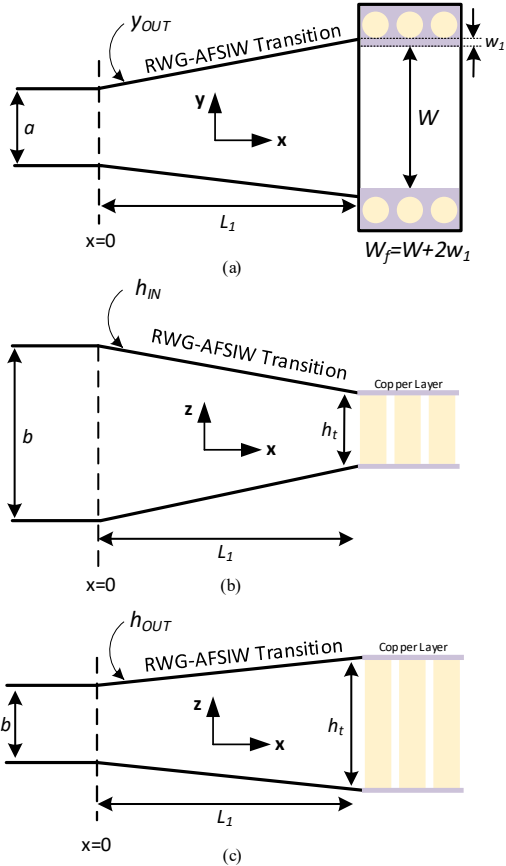

Fig. 2. The proposed linearly tapered transition between RWG and AFSIW in different scenarios (a) taper out in W_f (b) taper in h (c) taper out in h.

In transition design, the L_1 (mm) is a critical parameter as it balances the impedance matching and insertion loss; therefore,
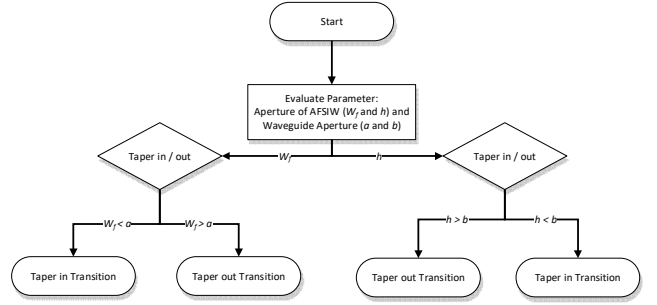

Fig. 3. Flow chart for deciding the taper out/in for transition design

in this work, its analytical expression related to f_c (GHz) of the transitions, which provides the optimum results for S_{11} and S_{21} is expressed as:

$$L_1 = 8.293 \times e^{-0.01881 \times f_c} \qquad (4)$$

IV. S-PARAMETER SIMULATION RESULTS

To validate the proposed design concept, several setups utilizing different waveguides, as shown in Fig. 4 (a)-(b) are used, and S_{11} and S_{21} results are generated, and their performances over various bands of operation are verified. The parameters like W and L_1 are determined using Eq. (1) and (4), and subsequently, $W_f = W + 2w_1$, where $w_1 = 0.26$mm (PCB edge tolerance) is used, and their values for different transitions are calculated and summarized in Table 1.
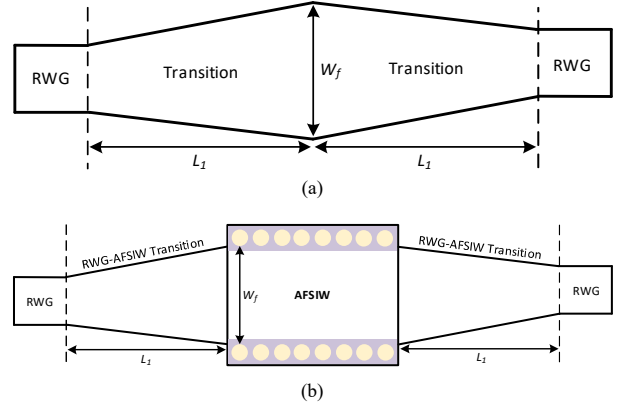

Fig. 4. Simulation setup of S_{11} and S_{21} for the proposed transition in different configurations (a) back-to-back (b) transmission system

Simulated results for S_{11} and S_{21} using the design parameters given in Table 1 are generated for back-to-back and transmission systems using Ansys HFSS, as shown in Fig. 5 and Fig.6, respectively. As observed from Fig. 5(a)-(b), which is compatible with WR-15, shows an average $S_{21}=-0.20$ dB over the frequency range of operation. In contrast, this value for WR-10 is found to be $S_{21}=-0.23$ dB, and in both cases, $S_{11}<-10$ dB. Similar results for the transmission system show the higher loss due to losses associated with AFSIW, which is more in the case of FR-4 ($\varepsilon_r=4.5$), as compared to Roger 5880 ($\varepsilon_r=2.2$) (See Fig. 6(a)-(b)). These results suggest the low insertion loss over the wideband for the proposed transition.
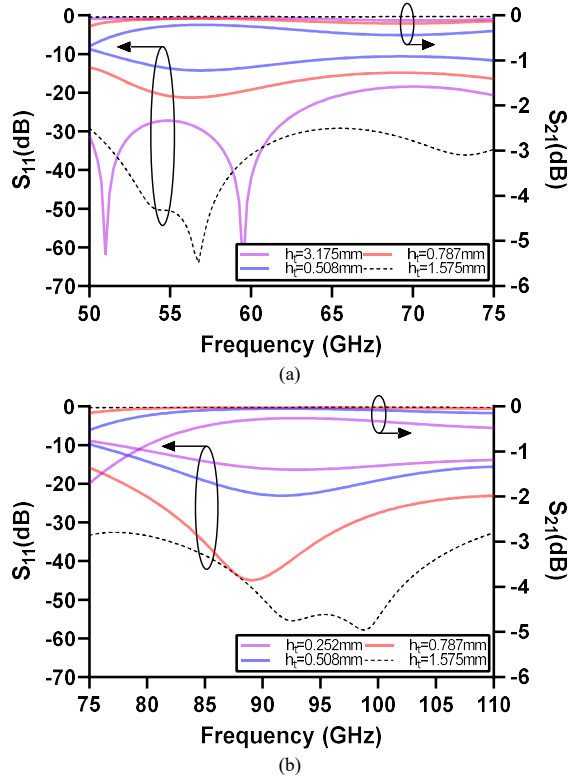
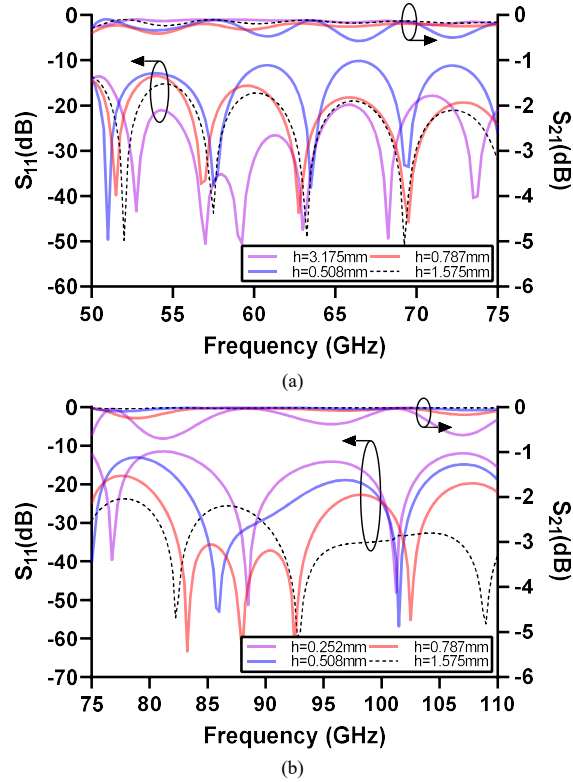Fig. 5. Simulation results in back-to-back configuration for S_{11} and S_{21} (a) WR-15 (b) WR-10

Fig. 6. Simulated results of S_{11} and S_{21} for transmission systems (a) WR-15 to AFSIW [FR-4] (b) WR-10 to AFSIW [Roger 5880]

Table 1. Design Parameters for Various Types of Transitions

Transition Type	W_f (mm)	L_1 (mm)	h (mm)
WR-15 to AFSIW	4.02	3.238	0.508-3.175
WR-10 to AFSIW	2.82	2.023	0.252-1.575

The W_f used for WR-15 to AFSIW transition using the parameters given in Table 1 verified the dominant mode TE_{10} of transmission at a center frequency of 62.5 GHz (See Fig. 7). Similar results in other cases were observed and not shown for simplicity.
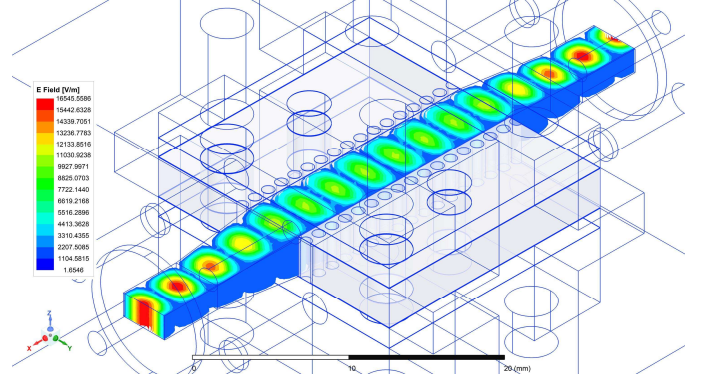

Fig. 7. Electric field vector distribution in TE_{10} mode at the centre frequency of 62.5 GHz for WR-15 to AFSIW transition.

V. PROTOTYPE OF THE PROPOSED TRANSITION

To verify the simulation results, a transmission system consisting of two back-to-back transitions with the AFSIW in between is fabricated on FR-4, compatible with WR-15, and parameters used are $W_f \cong 4.00$ mm, $L_1 \cong 3.2$, and $h= 3.175$ mm (See Fig. 8). It is measured using the Keysight PNA-X VNA N5247B (from 900 Hz to 67 GHz), extended up to 120 GHz using the extender N5295AX51. The loss of the WR-15 waveguide to the coaxial adapter is calibrated to measure the DUT (See Fig. 8) results accurately, and its operation from 50-75 GHz is experimentally verified (See Fig. 9).

VI. DISCUSSION AND COMPARISON WITH MEASURED RESULTS

The comparison of simulated and measured results of S_{11} and S_{21} are shown in Fig. 9 and found in close agreement. The simulated and measured S_{11} is found to be ≤ -10 dB for the frequency range from 50 to 75 GHz. The measured average S_{21} of the proposed transmission system is -0.48 dB, whereas the simulated result is -0.25 dB over the frequency of operation. The slight discrepancy between the simulation and measured results is due to the fabrication tolerance and the surface roughness. Table II summarizes the comparison between the proposed and available transitions in the literature in the operating frequency band. The results showed that the proposed transition using AFSIW demonstrated a wide bandwidth, and low insertion loss. The losses in FR-4 AFSIW were carefully de-embedded, and a close estimate for S21 for the transition was found to be -0.35 dB over the operating band.
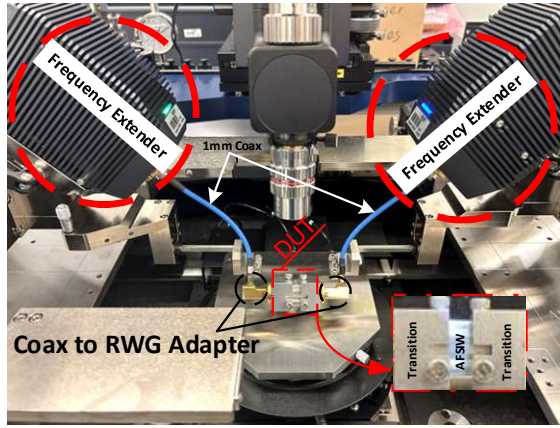
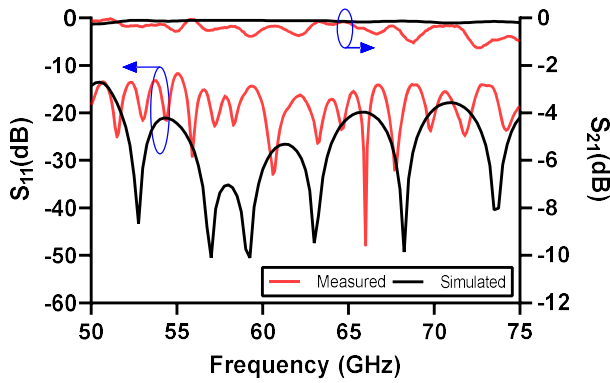Fig. 8. Fabricated prototype and measurement setup

Fig. 9. Comparison of measured and simulated S-parameters of the back-to-back transition.

Table 2. Performance Comparison of Proposed with existing Transition

Ref.	Transition Structure	S_{21} (dB)	BW (S_{11}@-10 dB) [GHz]
[12]	RWG-SIW	>-0.58	50.5-75.3
[13]	SIW-RWG	>-0.50	47.2 - 77.5
[14]	SIW-RWG	>-0.40	40-65
[This Work]	RWG-AFSIW	>-0.35	50-75

VII. CONCLUSIONS

A new wideband and low-loss transition from RWG to AFSIW is reported in this paper. A generalized design approach is followed, and transition length is analytically determined to balance impedance matching and insertion loss, thus simplifying the design process. The proposed design is prototyped in its transmission system configuration, and results for S_{11} and S_{21} in the 50-75 GHz range are experimentally verified. Various performances with similar works reported in the literature confirm the advantage of the proposed transition for developing low-cost multiple Gb/s data rate communication systems.

REFERENCES

[1] S. Mukherjee, ″Substrate Integrated Coaxial Line (SICL)- A new frontier for 5G millimeter wave communication, ″TechScape: The Science, Technology, and Education Journal, Vo.1 Issue 2, Dec 2020.

[2] Y. Xing and T. S. Rappaport, "Propagation Measurement System and Approach at 140 GHz-Moving to 6G and Above 100 GHz," 2018 IEEE Global Communications Conference, 2018, pp. 1-6.

[3] T. Martin, A. Ghiotto, A. Marque, T. P. Vuong, F. Lotz, P. Monteil, and L. Carpentier, "Broadband air-filled SIW to waveguide transition for interconnect, instrumentation and measurement applications," 2017 IEEE MTT-S International Microwave Workshop Series on Advanced Materials and Processes for RF and THz Applications (IMWS-AMP), 2017, pp. 1-3.

[4] I. L. D. Paula, S. Lemey, D. Bosman, Q. V. D. Brande, O. Caytan, J. Lambrecht, M. Cauwe, G. Torfs, and H. Rogier, ″Cost-Effective High-Performance Air-Filled SIW Antenna Array for the Global 5G 26 GHz and 28 GHz Bands,″ IEEE Antennas and Wireless Propagation Letters, 20(2), 194–198, 2021.

[5] F. Parment, A. Ghiotto, T. P. Vuong, J. M. Duchamp, and K. Wu, ″Air-filled substrate integrated waveguide for low-loss and high power-handling millimeter-wave substrate integrated circuits,″ IEEE Transaction Microwave Theory Technique, vol. 63, no. 4, pp. 1228-1238, Apr. 2015.

[6] T. Martin, A. Ghiotto and T. -P. Vuong, "Air-Filled Substrate Integrated Waveguide (AFSIW) Filter with Asymmetric Frequency Response," 2020 XXXIIIrd General Assembly and Scientific Symposium of the International Union of Radio Science, 2020, pp. 1-4.

[7] J. L. Cano, A. Mediavilla, and A. RY. Perez, ″Full-Band Air-Filled Waveguide-to-Substrate Integrated Waveguide Direct Transition″, IEEE Microwave, and Wireless Components Letters, 25(2), 79–81, 2015.

[8] L. Li, X. Chen, R. Khazaka, and K. Wu, ″A transition from substrate integrated waveguide (SIW) to rectangular waveguide,″ In Proc. Asia Pacific Microwave Conference (APMC'09), Singapore, Dec. 7–10, 2009, pp. 2605–2608.

[9] R. Glogowski, J.-F. Zürcher, C. Peixeiro, and J. R. Mosig, ″Broadband Ka-band rectangular waveguide to substrate integrated waveguide transition,″ Electronics Letter, vol. 49, no. 9, pp. 602–604, Apr. 2003.

[10] W. P. Ayeres, P. H. Vartanian, and A. L. Helgesson, ″Propagation in dielectric slab loaded rectangular waveguide,″ IRE Transaction Microwave Theory Technique, vol. MTT-6, no. 2, pp. 215–222, Feb. 1958

[11] K. Wu, D. Deslandes and Y. Cassivi, "The substrate integrated circuits - a new concept for high-frequency electronics and optoelectronics," 6th International Conference on Telecommunications in Modern Satellite, Cable and Broadcasting Service, TELSIKS 2003.

[12] Y. Li and K. -M. Luk, "A Broadband V-Band Rectangular Waveguide to Substrate Integrated Waveguide Transition," IEEE Microwave and Wireless Components Letters, vol. 24, no. 9, pp. 590-592, Sept. 2014.

[13] I. Mohamed, A. Sebak, ″Broadband Transition of Substrate-Integrated Waveguide-to-Air-Filled Rectangular Waveguide,″ IEEE Microwave and Wireless Components Letters, pp. 1–3, 2018.

[14] B. Wang, and H. Wong, ″Broadband Substrate Integrated Waveguide to Rectangular Waveguide Transition at V-Band,″ 2020 IEEE Asia-Pacific Microwave Conference (APMC), pp. 788-89.